International Journal of Thermophysics, Vol. 18, No. 5, 1997

An Analytic Expression for the First Shell of the Radial Distribution Function

H. Touba[1] **and G. A. Mansoori**[1, 2]

Received December 2, 1996

A simple analytical expression for the first shell of the radial distribution function (RDF) is proposed. This expression, which has only three adjustable parameters, satisfies all the limiting cases of the hard-sphere RDF at high temperatures, the ideal gas RDF at zero density, the dilute-gas RDF at low densities, and the location of the peak in the first shell. The only requirement is the introduction of a potential function into the model. This theory has been applied to the Lennard Jones, Kihara, and square-well pair intermolecular potential energy functions. The first-shell RDF results are in good agreement with the available computer simulation data for the RDF of the Lennard Jones fluid and the experimental data for argon. By introducing the radius of truncation for the RDF, it is shown that information on the first shell of the RDF is sufficient to predict macroscopic properties of fluids. Calculations of radii of truncation of RDF for various properties indicate that they are always in the range of the first shell of RDF.

KEY WORDS: Kihara potential; Lennard-Jones potential; radial distribution function; thermodynamic properties.

1. INTRODUCTION

The radial distribution function (RDF) is the most informative feature of the structure of a substance. It represents the probability of finding a molecule at a specified distance from an arbitrary central molecule and is denoted $g(r)$, r being the distance between molecules. In practice, we may think of $\rho g(r)$ as a representation of the local density of molecules in equilibrium at any distance r from the central molecule (ρ being the bulk density of the substance expressed as number of molecules per unit volume).

[1] Department of Chemical Engineering, University of Illinois at Chicago, 810 South Clinton, Chicago, Illinois 60607-7000, U.S.A.

[2] To whom correspondence should be addressed.

0195-928X/97/0900-1217$12.50/0

In the canonical ensemble, the radial distribution (pair correlation) function for a pure substance is defined as follows:

$$g_{ij}(r, \rho, T) = V^2(1-\delta_{ij}/N_j)/Q_c(T, V, N) \int \cdots \int e^{-\phi/kT} d\mathbf{r}_3 \cdots d\mathbf{r}_N \quad (1)$$

where T is the absolute temperature, V is the volume, $\mathbf{r}$ is the position vector, ϕ is the intermolecular potential energy function, δ_{ij} is the Kronecker delta, k is Boltzmann's constant, N is the number of molecules, and Q_c is the configurational integral which can be represented by the following equation:

$$Q_c(T, V, N) = \int \cdots \int e^{-\phi/kT} d\mathbf{r}_1 \cdots d\mathbf{r}_N \quad (2)$$

By using RDF, it is possible to calculate equilibrium properties (the isothermal compressibility, pressure, and internal energy) of a substance. The expressions for obtaining isothermal compressibility (κ_T), pressure (P), and internal energy (U) are

$$\kappa_T = -(1/V)(\partial V/\partial P)_T = (1/\rho)(\partial \rho/\partial P)_T$$

$$= 1/(\rho kT) + 4\pi/(kT) \int_0^\infty [\, g(r) - 1 \,]\, r^2\, dr \quad (3)$$

$$P = \rho kT - (2\pi\rho^2/3) \int_0^\infty g(r)\, \phi'(r)\, r^3\, dr \quad (4)$$

$$U = U_{ig} + 2N\pi\rho \int_0^\infty g(r)\, \phi(r)\, r^2\, dr \quad (5)$$

where U_{ig} is the ideal-gas internal energy.

In order to make these relationships dimensionless, we define $\rho^* \equiv \rho\sigma^3$, $T^* \equiv kT/\varepsilon$, $P^* \equiv P\sigma^3/\varepsilon$, $U^* \equiv (U - U_{ig})/(N\varepsilon)$, $\kappa_T^* \equiv \kappa_T \varepsilon/\sigma^3$, and $y \equiv r/\sigma$. σ and ε are the diameter and energy parameters of the potential energy function, respectively.

$$\kappa_T^* = 1/(\rho^* T^*) + (4\pi/T^*) \int_0^\infty [\, g(y) - 1 \,]\, y^2\, dy \quad (6)$$

$$P^* = \rho^* T^* - [2\pi^{*2}/(3\varepsilon)] \int_0^\infty g(y)\, \phi'(y)\, y^3\, dy \quad (7)$$

$$U^* = (2\pi\rho^*/\varepsilon) \int_0^\infty g(y)\, \phi(y)\, y^2\, dy \quad (8)$$

In this work, we have proposed a simple expression which can be used to predict the first shell of RDF of fluids with known intermolecular potential functions. It is shown that the first shell of RDF is the only information necessary in determining the equilibrium properties of substances. Hanley and Evans [1] and Mansoori and Ely [2] showed that the thermodynamic properties can be completely determined by interactions of relatively short range. Hanley and Evans could reproduce the experimental data using a distance of approximately 2.5 molecular diameter in their calculations for dense soft spheres. Here, it is determined that this distance (the radius of truncation of RDF) is a function of temperature and density, from which pressure, internal energy, and isothermal compressibility are calculated.

2. DEVELOPMENT OF AN ANALYTIC EXPRESSION FOR THE FIRST SHELL OF THE RDF

The limiting conditions that the radial distribution function has to satisfy are as follows.

(i) The case of an ideal gas, where RDF approaches unity.

(ii) The case of a dilute gas (dg), in which the RDF is represented by the following equation:

$$g_{\mathrm{dg}}(y) = \exp[-\beta\phi(y)] \tag{9}$$

where $\beta = 1/(kT)$.

(iii) The high-temperature limit, where the RDF can be represented by the hard-sphere RDF as derived by Wertheim's analytic expression [3].

(iv) The limit of zero molecular distance, where the RDF approaches zero.

(v) The limit of infinite distance between two molecules, where the RDF approaches unity.

We propose the following functional form for the first shell of the radial distribution function of fluids which possesses the correct shape of the first shell:

$$g(y) = m_1 g_{\mathrm{hs}}(1) \exp[-m_2\beta\phi(x)] + (1-m_1)\exp[-m_2\beta\phi(y) - c_1(y-d^*)]$$
$$\text{for} \quad 0 \leqslant y \leqslant d^* \tag{10}$$

$$g(y) = m_1 g_{\mathrm{hs}}(x) + (1-m_1)\exp[-m_2\beta\phi(y) - c_2(y-d^*)]$$
$$\text{for} \quad d^* \leqslant y < y_m \tag{11}$$

where $x \equiv r/d$, d is defined as the location of the maximum of the first shell, $d^* \equiv d/\sigma$, y_m is the location of the minimum in the RDF at the end of the first peak, $g_{hs}(x)$ is the first-shell hard-sphere RDF as derived by Wertheim and given in the Appendix, and $g_{hs}(1)$ is the hard-sphere RDF at the contact.

It should be also pointed out that the two parts of $g(y)$ for the first shell as given by Eqs. (10) and (11) converge to the following simple equation at the maximum of the first peak of the RDF (at $y = d^*$):

$$g(d^*) = m_1 g_{hs}(1) + (1 - m_1) \exp[-m_2 \beta \phi(d^*)] \tag{12}$$

The parameters c_1 and c_2 appearing in Eqs. (10) and (11) must be determined so that $g(y)$ will have a maximum at distance d^*, i.e.,

$$[\partial g(y)/\partial y]_{y=d^*} = 0$$

With this condition, the following analytic expressions for c_1 and c_2 will result:

$$c_1 = -m_1 m_2 \beta \phi'(1)\, g_{hs}(1)/\{d^*(1 - m_1) \exp[-m_2 \beta \phi(d^*)]\} - m_2 \beta \phi'(d^*) \tag{13}$$

$$c_2 = m_1 g'_{hs}(1)/\{d^*(1 - m_1) \exp[-m_2 \beta \phi(d^*)]\} - m_2 \beta \phi'(d^*) \tag{14}$$

$\phi'(1)$ and $g'_{hs}(1)$ are derivatives of the potential function and the RDF at contact, respectively. The expression for $g'_{hs}(1)$ is derived and reported in the Appendix based on Wertheim's hard-sphere RDF at contact.

In order to satisfy the limiting conditions imposed on the RDF due to temperature and density variations (conditions i, ii, and iii) and to possess the correct temperature and density dependencies, the parameters d^*, m_1, and m_2 in the above equations are expressed as functions of the reduced temperature, T^*, and the reduced density, ρ^*, as indicated below:

$$d^* = R_m \exp(-\xi_1 \rho^{*2} T^{*0.5}) \tag{15}$$

$$m_1 = \exp[-\xi_2/(\rho^* T^*)] \tag{16}$$

$$m_2 = \exp[\xi_3 \rho^* (1 - 1/T^*)] \tag{17}$$

where ξ_1, ξ_2, and ξ_3 are adjustable parameters and R_m is the location of the dilute-gas RDF peak. Considering that Eq. (9) expresses the dilute-gas RDF, the parameter R_m can be calculated using the condition $[\partial \exp[-\beta \phi(y)]/\partial y]_{y=R_m} = 0$, which will be reduced to the following expression:

$$[\partial \phi(y)/\partial y]_{y=R_m} = \phi'(y = R_m) = 0 \tag{18}$$

According to Eq. (16), as the temperature approaches infinity, the parameter m_1 becomes unity. Substituting $m_1 = 1$ into Eq. (11), it reduces to $g_{hs}(x)$, which is the limiting case of the hard-sphere RDF. For the case where the density is very low, according to Eqs. (13)–(18), $m_1 = c_1 = c_2 = 0$ and $m_2 = 1$. Therefore, Eqs. (10) and (11) reduce to Eq. (9), which is the dilute-gas RDF.

Equations (10) and (11), when joined with the expressions for c_1, c_2, d^*, m_1, and m_2 given by Eqs. (13)–(18), can be used for the calculation of the first shell of RDF of simple fluids with known potential energy functions. In what follows, we apply these analytic expressions for the calculation of the first shell of RDF of various potential energy functions. As will be shown, we are able to correlate all the available simulation and experimental first-shell RDF data of simple fluids by these expressions. It should be pointed out that the three adjustable parameters ξ_1, ξ_2, and ξ_3 are dimensionless and they remain constant for any simple fluid.

3. APPLICATION TO VARIOUS POTENTIAL ENERGY FUNCTIONS

3.1. The Lennard–Jones Potential Function

The Lennard–Jones potential function, which has been widely studied in statistical mechanics, is one of the simplest model potential functions representing both the repulsive and attractive features of a real simple substance. Several investigators have attempted to fit simulation data for the Lennard–Jones fluid to analytical expressions. Goldman [4] proposed an expression with 108 adjustable parameters for the RDF of pure Lennard–Jones fluids and was able to reproduce Verlet's simulation data [5]. Recently, Matteoli and Mansoori [6] presented expressions for the Lennard–Jones RDF which require 21 parameters.

The analytical equations, Eqs. (10) and (11), presented in this report for the first shell of RDF have only three adjustable parameters. In the case of the Lennard–Jones fluid $\phi(y)$, $\phi(x)$, $\phi(d^*)$, $\phi'(d^*)$, $\phi'(1)$, and R_m appearing in Eqs. (10)–(15) are as indicated below:

$$\phi(y) = 4\varepsilon(1/y^{12} - 1/y^6) \tag{19}$$

$$\phi(x) = 4\varepsilon(1/x^{12} - 1/x^6) \tag{20}$$

$$\phi(d^*) = 4\varepsilon(1/d^{*12} - 1/d^{*6}) \tag{21}$$

$$\phi'(d^*) = -(24\varepsilon/d^*)(2/d^{*12} - 1/d^{*6}) \tag{22}$$

$$\phi'(1) = -24\varepsilon \tag{23}$$

$$R_m = 2^{1/6} \tag{24}$$

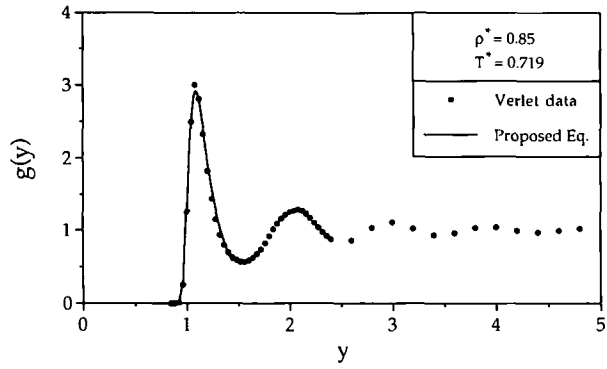

Fig. 1. Comparison of the proposed model for the first shell of the RDF and the simulation data obtained by Verlet [5] at $\rho^* = 0.85$ and $T^* = 0.719$.

The only adjustable parameters, ξ_1, ξ_2, and ξ_3, in Eqs. (15)–(17) have been obtained by fitting the 25 set of molecular dynamic simulation data reported by Verlet [5] for the first shell of RDF.

$$\xi_1 = 0.0483, \qquad \xi_2 = 4.930, \qquad \xi_3 = 0.680$$

Figures 1 to 4 represent comparisons between the simulation data of Verlet and the calculated RDF based on the proposed model at different T^* and ρ^* values. According to these figures the proposed model yields good agreement with the simulated data.

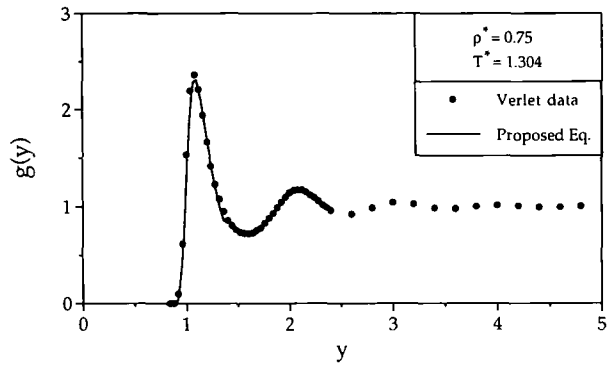

Fig. 2. Comparison of the proposed model for the first shell of the RDF and the simulation data obtained by Verlet [5] at $\rho^* = 0.75$ and $T^* = 1.304$.

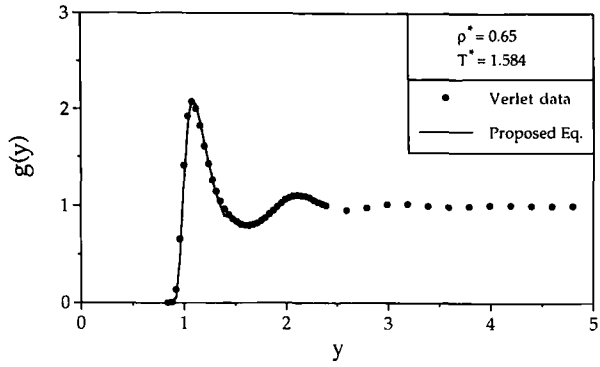

Fig. 3. Comparison of the proposed model for the first shell of the RDF and the simulation data obtained by Verlet [5] at $\rho^* = 0.65$ and $T^* = 1.584$.

Yarnell et al. [7] obtained the radial distribution function of liquid argon at 85 K from neutron scattering measurements. Later Soper [8] reevaluated the radial distribution of argon, which was quite close to the measured RDF data of Yarnell et al. [7]. In Fig. 5, we compare the first-shell RDF data of argon measured by Yarnell et al. [7] with the proposed $g(r)$ model using the Lennard–Jones parameters $\sigma = 3.405$ Å and $\varepsilon/k = 119.8$ K determined by Levelt [9]. According to this figure, there is a good agreement between the calculations and the experimental data. A similar comparison can be made using the argon Lennard–Jones potential parameters $\sigma = 3.400$ Å and $\varepsilon/k = 116.8$ K determined by Boublik [10].

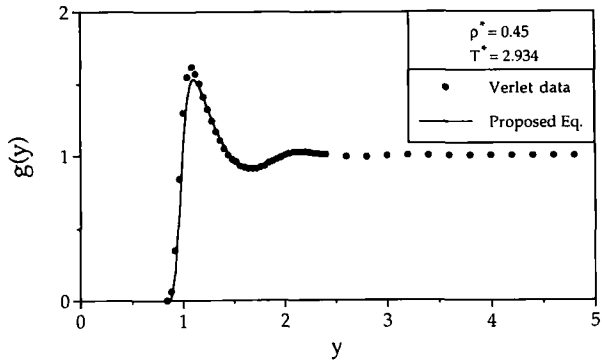

Fig. 4. Comparison of the proposed model for the first shell of the RDF and the simulation data obtained by Verlet [5] at $\rho^* = 0.45$ and $T^* = 2.934$.

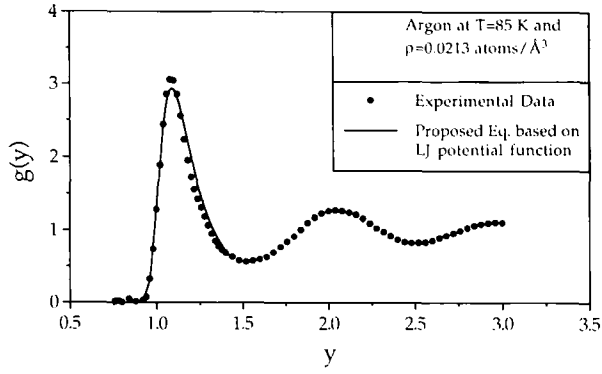

Fig. 5. Comparison of the proposed model based on the LJ potential function and the experimental RDF for argon at 85 K by Yarnell et al. [7].

However, the difference is not so noticeable in the graphical representations using the two sets of potential parameters.

3.2. The Kihara Potential Function

The Kihara potential function is a more realistic pair-potential model for fluids than the Lennard–Jones potential function to account for the intermolecular forces. It is assumed that each molecule has an impenetrable hard convex core which depends on the shortest distance between the two molecules. In the special case where the intermolecular orientation is of no importance, the core is a sphere with diameter δ. In order to apply the proposed first-shell RDF model to the Kihara potential, we can derive the following expressions for $\phi(y)$, $\phi(x)$, $\phi(d^*)$, $\phi'(d^*)$, $\phi'(1)$, and R_m:

$$\phi(y) = 4\varepsilon\{[(1-\delta^*)/(y-\delta^*)]^{12} - [(1-\delta^*)/(y-\delta^*)]^6\} \tag{25}$$

$$\phi(x) = 4\varepsilon\{[(1-\delta^*/d^*)/(x-\delta^*/d^*)]^{12} - [(1-\delta^*/d^*)/(x-\delta^*/d^*)]^6\} \tag{26}$$

$$\phi(d^*) = 4\varepsilon\{[(1-\delta^*)/(d^*-\delta^*)]^{12} - [(1-\delta^*)/(d^*-\delta^*)]^6\} \tag{27}$$

$$\phi'(d^*) = [-24\varepsilon/(d^*-\delta^*)]\{2[(1-\delta^*)/(d^*-\delta^*)]^{12} - [(1-\delta^*)/(d^*-\delta^*)]^6\} \tag{28}$$

$$\phi'(1) = -24\varepsilon/(1-\delta^*/d^*) \tag{29}$$

$$R_m = \delta^* + 2^{1/6}(1-\delta^*) \tag{30}$$

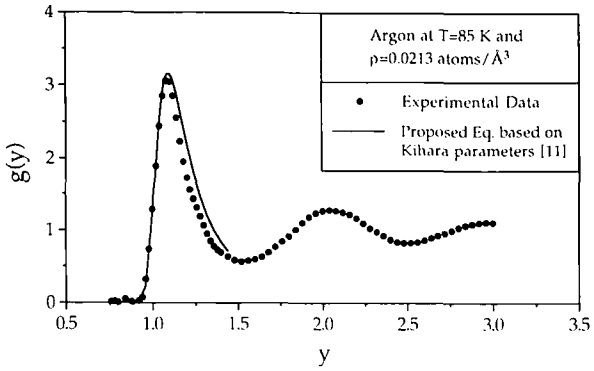

Fig. 6. Comparison of the proposed model based on the Kihara potential parameters in Ref. 11 and the experimental RDF for argon at 85 K by Yarnell et al. [7].

where $\delta^* = \delta/\sigma$. The parameters ξ_1, ξ_2, and ξ_3 in Eqs. (15) to (17) are assumed to have the same values as in the Lennard–Jones case.

Figure 6 represents comparisons between the experimental RDF of liquid argon at 85 K determined by Yarnell et al. [7] and the proposed $g(r)$ obtained by using the Kihara parameters [11], $\sigma = 3.314$ A, $\varepsilon/k = 146.52$ K, and $\delta = 0.121$ A. The agreement of the experimental data and the calculated RDF depends on the choice of the potential parameters. If the Kihara potential parameters $\sigma = 3.344$ A, $\varepsilon/k = 143.26$ K, and $\delta = 0.334$ A reported by Tee et al. [12] are used in the proposed RDF, as in Fig. 7, we find a better agreement with the experimental data of Yarnell et al. [7].

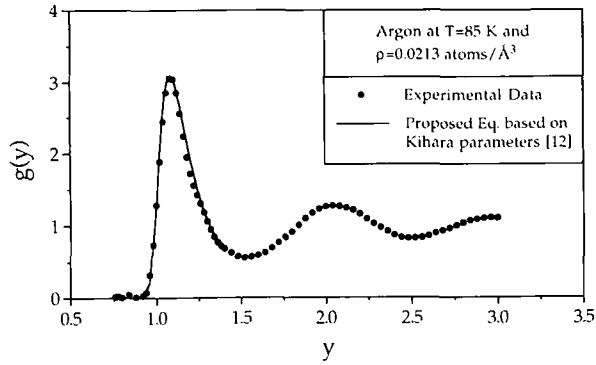

Fig. 7. Comparison of the proposed model based on the Kihara potential parameters in Ref. 12 and the experimental RDF for argon at 85 K by Yarnell et al. [7].

In comparing this figure with Fig. 5 in which the same experimental data were compared with the first-shell Lennard–Jones model calculation, we conclude that the Kihara potential complies better with the proposed model for argon.

3.3. The Square-Well Potential Function

The square-well potential function also has both repulsive and attractive forces.

$$\begin{aligned} \phi(y) &= \infty && \text{for} \quad y < 1 \\ \phi(y) &= -\varepsilon && \text{for} \quad 1 < y < \lambda \\ \phi(y) &= 0 && \text{for} \quad \lambda < y \end{aligned} \tag{31}$$

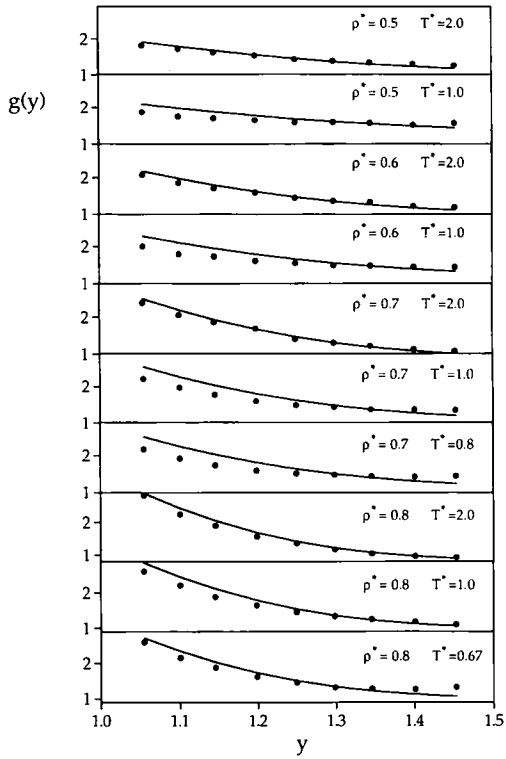

Fig. 8. Comparison between the proposed RDF using the square-well potential function (solid lines) and the Monte Carlo simulation data [13] for $\lambda = 1.5$ (filled circles).

where λ is the attractive diameter which represents the width of the well. We may assume the following simple expression for the first shell of the radial distribution function of the square-well model, which satisfies all the limiting conditions imposed on it:

$$g(y) = m_1 g_{hs}(x) + (1 - m_1) \exp(m_2/T^*) \qquad \text{for} \quad 1 < y < \lambda \qquad (32)$$

where $x \equiv y/d^*$, $d^* = 1$, $m_1 = \exp[-\xi_2/(\rho^* T^*)]$, and $m_2 = \exp[\xi_3 \rho^* (1 - 1/T^*)]$. The adjustable parameters ξ_2 and ξ_3 are determined by fitting Eq. (32) to the available Monte Carlo simulation data [13], which is for $\lambda = 1.5$.

$$\xi_2 = 0.142, \qquad \xi_3 = 1.675$$

Figure 8 represents comparisons between all the Monte Carlo simulation data and the proposed RDF that is obtained by using the square-well potential function. Although the square-well first shell RDF is simpler than the Lennard–Jones and Kihara first-shell RDFs, the results of the proposed method for the square well are not as good as those of the Lennard–Jones and Kihara.

4. SUFFICIENCY OF THE FIRST SHELL OF THE RDF IN PROPERTY CALCULATIONS

In this report, we examine the sufficiency of the first shell for the calculation of thermodynamic properties. In doing so, we utilize the simulation data, which include isothermal compressibility, pressure, and internal energy, for the Lennard–Jones fluid to calculate the distance at which the RDF could be truncated. In all cases studied, it is shown that the radius of truncation is located inside the first shell of the RDF.

4.1. Isothermal Compressibility

To calculate the isothermal compressibility using the RDF, we demonstrate here that the information on the first shell of RDF is sufficient. In order to express the isothermal compressibility using only the first shell of the RDF, we introduce R_κ, the radius of truncation of the RDF. The integral in Eq. (6) can be written in the following form:

$$\int_0^\infty [g(y) - 1]\, y^2\, dy = \int_0^{R_\kappa} [g(y) - 1]\, y^2\, dy + \int_{R_\kappa}^\infty [g(y) - 1]\, y^2\, dy \qquad (33)$$

R_κ can be chosen such that the second integral in Eq. (33) disappears, i.e.,

$$\int_{R_\kappa}^{\infty} [\, g(y) - 1 \,]\, y^2\, dy = 0 \tag{34}$$

In general, Eq. (34) has several roots for R_κ. However, we impose the constraint that R_κ has to be within the first shell of RDF. Figure 9 represents schematically the value of R_κ which gives rise to the equality of dashed areas above and below the horizontal axis to the right of R_κ. Since $g(y)$ is a function of temperature and density, R_κ is also a function of temperature and density.

Considering Eq. (34), we substitute Eq. (33) into Eq. (6).

$$\kappa_T^* = 1/(\rho^* T^*) + (4\pi/T^*) \int_0^{R_\kappa} [\, g(y) - 1 \,]\, y^2\, dy$$

$$= 1/(\rho^* T^*) + (4\pi/T^*) \left[\int_0^{R_\kappa} g(y)\, y^2\, dy - R_\kappa^3/3 \right] \tag{35}$$

In order to obtain R_κ, we have derived the isothermal compressibility from the simulation data of the Lennard–Jones fluid through the correlation proposed by Johnson et al. [14]. Their correlation is considered to be quite accurate for pressure calculations. However, its accuracy for isothermal compressibility cannot be investigated due to the lack of simulation data. Variations of R_κ with density and temperature are illustrated in Fig. 10. According to this figure, for all the temperatures and densities for which the

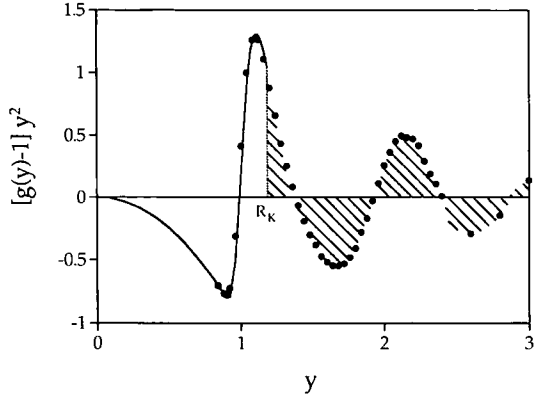

Fig. 9. Radius of truncation R_κ for the isothermal compressibility integral $[\, g(y) - 1 \,]\, y^2$.

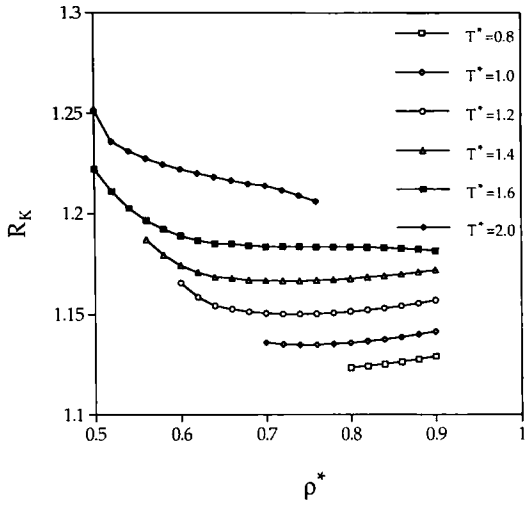

Fig. 10. Variations of the radius of truncation R_K with temperature and density for Lennard–Jones fluids.

correlation by Johnson et al. [14] is valid, the radius of truncation of RDF is within the first shell.

4.2. Pressure

The same procedure as for R_K can be applied for pressure to find the radius of truncation of the radial distribution function, R_P, for pressure calculations. The integral in Eq. (7) can be split as follows:

$$\int_0^\infty g(y)\,\phi'(y)\,y^3\,dy = \int_0^{R_P} g(y)\,\phi'(y)\,y^3\,dy + \int_{R_P}^\infty \phi'(y)\,y^3\,dy + \int_{R_P}^\infty [g(y)-1]\,\phi'(y)\,y^3\,dy \tag{36}$$

R_P is chosen such that the last integral in Eq. (36) vanishes, i.e.,

$$\int_{R_P}^\infty [g(y)-1]\,\phi'(y)\,y^3\,dy = 0 \tag{37}$$

Figure 11 depicts how the equal areas above and below the horizontal axis to the right of R_P cancel each other.

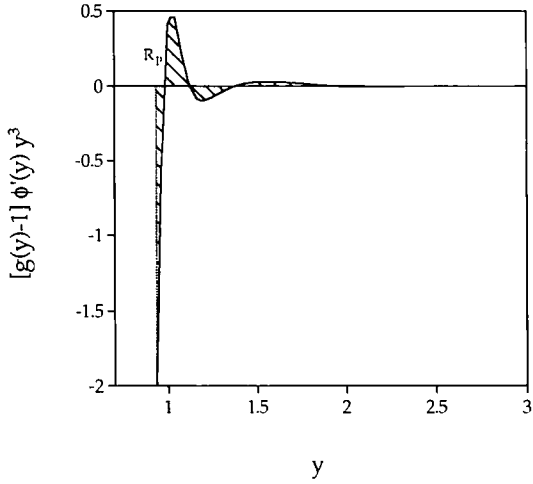

Fig. 11. Radius of truncation R_P for pressure integrand $[g(y)-1]\,\phi'(y)\,y^3$.

Considering Eq. (37) and applying the Lennard–Jones potential function, we get the following equation for pressure:

$$P^* = \rho^* T^* = 16\pi\rho^{*2}\left\{\int_0^{R_P} g(y)(2/y^{10} - 1/y^4)\,dy + 2/(9R_P^9) - 1/(3R_P^3)\right\} \quad (38)$$

In order to calculate R_P, we have utilized the correlation proposed by Johnson et al. [14] and the Lennard–Jones fluid simulation data for pressure as given by Verlet [15]. Figure 12 and Table I show how R_P changes with the density and temperature. According to Fig. 12 and Table I, the radii of truncation of the RDF are within the first shell for all the temperatures and densities reported.

4.3. Internal Energy

In the case of the internal energy, the integral in Eq. (8) is written as

$$\int_0^\infty g(y)\,\phi(y)\,y^2\,dy = \int_0^{R_U} g(y)\,\phi(y)\,y^2\,dy + \int_{R_U}^\infty \phi(y)\,y^2\,dy + \int_{R_U}^\infty [g(y)-1]\,\phi(y)\,y^2\,dy \quad (39)$$

Table I. Calculated Radii of Truncation, R_P and R_U, versus ρ^* and T^* from Simulated Data for Pressure and Internal Energy[a]

ρ^*	T^*	R_P	R_U
0.880	1.095	0.9145	1.1405
0.880	0.940	0.9222	1.1475
0.880	0.591	0.9422	1.1957
0.850	2.889	0.8778	1.0703
0.850	2.202	0.8895	1.1062
0.850	1.214	0.9154	1.1712
0.850	1.128	0.9189	1.1741
0.850	0.880	0.9303	1.1744
0.850	0.782	0.9356	1.1740
0.850	0.786	0.9355	1.1757
0.850	0.760	0.9370	1.1749
0.850	0.719	0.9400	1.1761
0.850	0.658	0.9435	1.1781
0.850	0.591	0.9495	1.1814
0.750	2.849	0.8913	1.1106
0.750	1.304	0.9280	1.1900
0.750	1.069	0.9371	1.1826
0.750	1.071	0.9372	1.1797
0.750	0.881	0.9476	1.1717
0.750	0.827	0.9517	1.1730
0.650	2.557	0.9082	1.1625
0.650	1.585	0.9322	1.1975
0.650	1.036	0.9535	1.1747
0.650	0.900	0.9612	1.1684
0.550	2.645	0.9176	1.1967
0.543	3.260	0.9059	1.1563
0.543	1.404	0.9480	1.1970
0.543	1.326	0.9511	1.1922
0.500	1.360	0.8969	1.1998
0.450	4.625	0.8997	1.0912
0.450	2.935	0.9231	1.2086
0.450	1.744	0.9499	1.2126
0.450	1.764	0.9492	1.2116
0.450	1.710	0.9493	1.2290
0.450	1.552	0.9462	1.2124
0.400	1.462	0.9644	1.2266
0.400	1.424	0.9646	1.2229
0.350	1.620	0.9635	1.2248
0.350	1.418	0.9694	1.1560

[a] From Ref. 15.

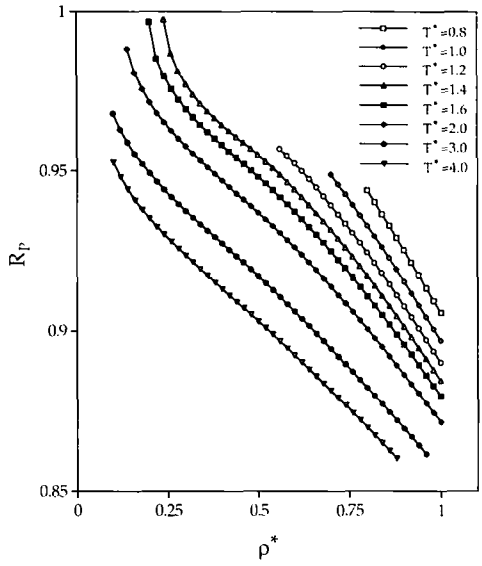

Fig. 12. Variations of the radius of truncation R_p with temperature and density for Lennard Jones fluids.

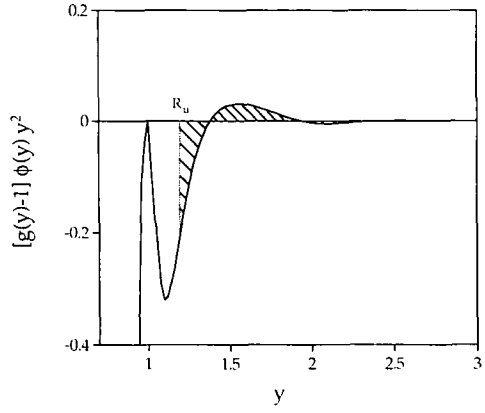

Fig. 13. Radius of truncation R_u for internal energy integrand $[g(y)-1]\phi(y)y^2$.

In the same way as for the isothermal compressibility and pressure, R_U is chosen such that the last integral in Eq. (39) disappears, i.e.,

$$\int_{R_U}^{\infty} [\, g(y) - 1 \,]\, \phi(y)\, y^2\, dy = 0 \tag{40}$$

Figure 13 presents schematically the preceding integral and the equality of areas above and below the horizontal axis to the right of R_U.

Applying the Lennard–Jones potential function, we conclude that

$$U^* = 8\pi\rho^* \left\{ \int_0^{R_U} g(y)(1/y^{10} - 1/y^4)\, dy + 1/(9R_U^9) - 1/(3R_U^3) \right\} \tag{41}$$

In order to determine R_U, we have used the correlation of Johnson et al. [14] and the internal energy data of Verlet [15]. Variations of R_P with density and temperature are illustrated in Fig. 14 and in Table I. According to Fig. 14 and Table 1, for all the temperatures and densities reported, the radius of truncation of the RDF for internal energy calculation is within the first shell.

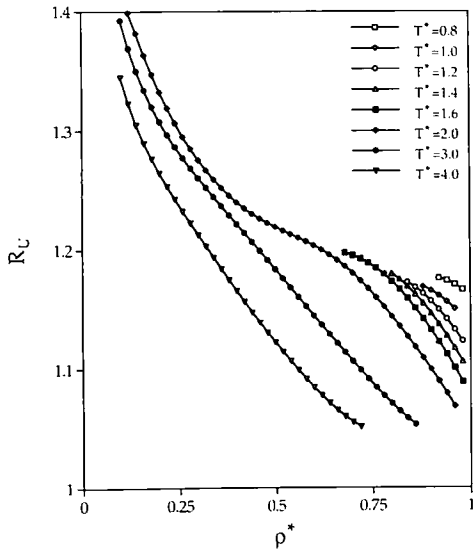

Fig. 14. Variations of the radius of truncation R_U with temperature and density for Lennard Jones fluids.

5. CONCLUSION

We have presented a simple model for determining the first shell of the RDF provided the potential energy function is known. The proposed model conforms to the limiting cases of ideal gas, dilute gas, and the hard-sphere limit. It also has an appropriate temperature and density dependence which satisfies all the related variations of the first-shell RDF. It has three adjustable parameters which have to be determined from the simulation or experimental RDF first-shell data. The present model is tested versus the first-shell RDF data for the Lennard–Jones, Kihara, and square-well fluids. Moreover, the proposed model is tested versus the experimental results for the argon RDF. Good agreement was obtained in most of the cases studied over a broad range of density and temperature. In order to express the significance of the first shell of the RDF, we have examined the sufficiency of the first shell of RDF for thermodynamic property calculations. It is shown that, for all the available simulated Lennard–Jones fluid data, the radius of truncation of the RDF is located within the first shell. As demonstrated by Figs. 10–14 and discussed above for calculating internal energy, pressure, and isothermal compressibility, the radius of truncation of the RDF is always located inside the first shell of the RDF. This indicates that for thermodynamic property calculations which start with the radial distribution function, information on the first shell of the RDF seems to be sufficient.

APPENDIX: HARD-SPHERE RADIAL DISTRIBUTION FUNCTION

Wertheim's analytical solution of the Percus–Yevick equation for the first shell of the hard-sphere radial distribution function [3] is

$$g_{hs}(x) = [(H_0 + H_1 + H_2)\exp(A_1) + 2\exp(A_3)(D_1 \cos A_2 - D_2 \sin A_2)]/[3x(1-\eta)^2] \quad \text{(A1)}$$

where $\eta = \pi\rho\, d^3/6$ is the dimensionless density or packing fraction, and parameters A_1, A_2, A_3, D_1, D_2, H_0, H_1, and H_2 are defined as follows:

$$A_1 = [2\eta/(1-\eta)](x-1)(-1+x_+ + x_-) \quad \text{(A2)}$$

$$A_2 = [2\eta/(1-\eta)](x-1)(3^{1/2}/2)(x_+ - x_-) \quad \text{(A3)}$$

$$A_3 = [2\eta/(1-\eta)](x-1)[-1-0.5(x_+ + x_-)] \quad \text{(A4)}$$

$$D_1 = H_0 - 0.5(H_1 + H_2) \tag{A5}$$

$$D_2 = (3^{1/2}/2)(H_1 - H_2) \tag{A6}$$

$$H_0 = 1 + 0.5\eta \tag{A7}$$

$$H_1 = -[x_-^2(1 - 3\eta - 4\eta^2) + x_+(1 - 2.5\eta^2)]/[4\eta(f^2 + \tfrac{1}{8})^{1/2}] \tag{A8}$$

$$H_2 = [x_+^2(1 - 3\eta - 4\eta^2) + x_-(1 - 2.5\eta^2)]/[4\eta(f^2 + \tfrac{1}{8})^{1/2}] \tag{A9}$$

f, x_+, and x_- in the preceding equations are defined as

$$f = (3 + 3\eta - \eta^2)/4\eta^2 \tag{A10}$$

$$x_+ = [f + (f^2 + \tfrac{1}{8})^{1/2}]^{1/3} \tag{A11}$$

$$x_- = [f - (f^2 + \tfrac{1}{8})^{1/2}]^{1/3} \tag{A12}$$

In the case where $x = 1$ (or $r = d$), Eq. (A1) reduces to

$$g_{hs}(1) = (1 - \eta/2)/(1 - \eta)^2 \tag{A13}$$

The maximum of the hard-sphere RDF at $r = d$ (or $x = 1$) can be obtained by taking the derivative of Eq. (A1) with respect to x.

$$g'_{hs}(1) = -4.5\eta(1 + \eta)/(1 - \eta)^3 \tag{A14}$$

ACKNOWLEDGEMENT

The authors are indebted to the National Science Foundation (Grant CTS-9108595) for supporting this research.

REFERENCES

1. H. J. M. Hanley and D. J. Evans, *Int. J. Thermophys.* **2**:1 (1981).
2. G. A. Mansoori and J. F. Ely, *Fluid Phase Equil.* **22**:253 (1985).
3. M. S. Wertheim, *Phys. Rev. Lett.* **10**:321 (1963).
4. S. Goldman, *J. Phys. Chem.* **83**:3033 (1979).
5. L. Verlet, *Phys. Rev.* **165**:201 (1968).
6. E. Matteoli and G. A. Mansoori, *J. Chem. Phys.* **103**:4672 (1995).
7. J. L. Yarnell, M. J. Katz, R. G. Wenzel, and S. H. Koenig, *Phys. Rev. A* **7**:2130 (1973).
8. A. K. Soper, *Chem. Phys.* **107**:61 (1986).
9. J. M. H. Levelt, *Physica* **26**:361 (1960).
10. T. Boublik, *J. Chem. Phys.* **87**:1751 (1987).
11. L. L. Lee, *Molecular Thermodynamics of Nonideal Fluids* (Butterworths, Boston 1988).
12. L. S. Tee, S. Gotoh, and W. E. Stewart, *Ind. Eng. Chem. Fund.* **5**:363 (1966).
13. D. Henderson, W. G. Madden, and D. Fitts, *J. Chem. Phys.* **64**:5026 (1976).
14. J. K. Johnson, J. A. Zollweg, and K. E. Gubbins, *Mol. Phys.* **78**:591 (1993).
15. L. Verlet, *Phys. Rev.* **159**:98 (1967).